IEEE/CSC & ESAS EUROPEAN SUPERCONDUCTIVITY NEWS FORUM (ESNF), No. 11, January 2010
Published in *Journal of Physics Conf. Series* (*SuST*) **234**, 042029 (2010)

Energy relaxation time in NbN and YBCO thin films under optical irradiation

D Rall[1,2], P Probst[1], M Hofherr[1], S Wünsch[1], K Ilin[1], U Lemmer[2] and M Siegel[1]
[1] Institut für Mikro- and Nanoelektronische Systeme, University of Karlsruhe, Hertzstrasse 16, 76187 Karlsruhe, Germany
[2] Lichttechnisches Institut, University of Karlsruhe, Engesserstrasse 13, 76131 Karlsruhe, Germany

E-mail: dagmar.rall@lti.uni-karlsruhe.de, p.probst@ims.uni-karlsruhe.de

Abstract. A systematic study of energy relaxation processes in thin NbN and YBCO films on sapphire substrates has been performed by means of the frequency domain technique. The magnetron sputtered NbN films of 3 nm to 22 nm thickness and pulsed-laser deposited YBCO with thicknesses between 20 nm and 45 nm were excited by amplitude-modulated optical radiation (λ=850 nm). The response spectra were analyzed on basis of the two-temperature model of the energy dynamics in the interacting electron and phonon subsystems at quasi-equilibrium conditions. An increase of the energy relaxation time with increasing film thickness has been obtained for both NbN and YBCO thin film samples. We argue that for both materials this characteristic time is mostly defined by phonon transfer through the film-substrate interface.

1. Introduction

Highly sensitive and ultra-fast Hot-Electron Bolometer (HEB) detectors are currently of high concern in research aiming to develop detectors for spectroscopy, security and astronomy applications, especially in the THz frequency range. Detectors made from low-temperature superconducting materials such as niobium nitride (NbN) meet the requirement of high sensitivity up to the single photon regime. High-T_c materials like $YBa_2Cu_3O_{7-\delta}$ (YBCO) are suitable for the development of very fast detectors since their electron-phonon interaction time is about one magnitude smaller ($\tau_{ep} \approx$ 1-2 ps for YBCO [1]) compared to low-T_c materials ($\tau_{ep} \approx$ 10 ps for NbN at 10.5 K [2]). Another advantage of high-temperature superconductors is the use of liquid nitrogen for device operation allowing for much more economic applications.

The photoresponse in superconductors already attracted considerable attention and was investigated by several groups either by using optical pulses [1], [3], [4], [5] or amplitude modulated THz radiation [1], [6], [7]. In both cases the experiments were carried out in the non-equilibrium regime due to high laser pulse energy or high local oscillator power, respectively. Also, for sub-THz radiation a contribution from vortex motions to the response was observed for both materials [8], [9], [10], which have a strong influence on the intermediate frequency bandwidth of HEB mixers made from NbN and YBCO films. In order to investigate the speed-limiting process of detectors, the phonon escape rate from the film into the substrate, it is essential to study the energy relaxation processes under quasi-equilibrium conditions, i.e. for small excitation energies, when a change of the effective temperatures of the electron and phonon subsystems is much smaller than the operation temperature. Therefore, we

performed our measurements using optical radiation to avoid any influence of moving vortices. The frequency domain technique supports the detailed determination of the energy relaxation time at quasi-equilibrium conditions, since very high resolution can be reached even at low excitation power.

In this report, we aim to compare NbN and YBCO thin films, which are very different in their material composition, microstructure and electron and phonon properties, as two representatives for similar application areas. We present a systematic study of the response spectra to optical radiation for both materials and analyse their dependence on film thickness.

2. Fabrication and characterization of NbN and YBCO samples

The YBCO and NbN samples have the same detector geometry consisting of an area of parallel and equally spaced stripes. The stripes are embedded into gold contact pads of a coplanar design, which also serves to reflect the photons incident on the contact areas, so that the absorbed radiation is confined to the central part of the sample.

The NbN thin films were deposited by DC reactive magnetron sputtering of a Nb target in an Ar/N_2 atmosphere. As substrate, one-side polished R-plane sapphire was used and heated to 750°C during the deposition of 3 nm to 22 nm thick films (for more details on NbN thin film fabrication and properties see [11]). To pattern the central structure of the NbN samples, standard photolithography was used with subsequent reactive ion etching. After a second lithography step, the sample surface was cleaned *in-situ* with an ion beam before sputtering the gold contacts on top of the NbN films.

The YBCO thin films were fabricated using on-axis pulsed-laser deposition (PLD) technique. A 50 nm thick CeO_2 buffer layer was deposited on sapphire substrate at a temperature of 820°C. The YBCO layers with different thicknesses between 10 nm and 100 nm were deposited on top of the CeO_2 layer. Finally, a 60 nm Au protection layer was grown *in-situ* using the same PLD technique. The Au contact pads of the YBCO films were patterned by standard photolithography and argon ion milling. To pattern the active/detecting area of the YBCO film wet etching with an I_2-KI solution was used.

The fabricated samples were characterized in a DC setup using a quasi four-probe measurement configuration. The temperature dependence of the resistance showed for the thin NbN films a very steep superconducting transition of about 1 K in width, resulting in a sharp peak in the derivative dR/dT of up to 1000 Ω/K. For YBCO, the width of the superconducting transition was broader resulting in much lower dR/dT values up to 40 Ω/K.

The critical temperature T_c is defined as the highest temperature at which the resistance reaches zero value. The T_c values of the NbN films with thicknesses $d \geq 10$ nm increased gradually from about 15.5 K up to 16.2 K for the thickest films which is only on 1 K lower than T_c of the bulk NbN samples. For the films thinner than 10 nm we observed a strong reduction of T_c down to 12.5 K for the thinnest 3 nm film. The YBCO films with $d \geq 30$ nm showed almost a constant value of T_c about 83 K. The critical temperature of thinner films decreased significantly down to 25 K for the 13 nm thick film. The decrease of T_c with decreasing film thickness is discussed in detail in [12], [13] for NbN and in [8] for YBCO thin films.

3. Experimental setup

As described above, the contact pads of the device are designed in a coplanar waveguide layout matched to 50 Ω impedance. The samples are bonded with indium to a coplanar bias-tee circuit on the sample holder. The modulated laser light is generated by a commercial Toptica laser system [14] of two temperature-controlled diode lasers at 850 nm wavelength coupled into the same optical glass fiber. The radiation frequencies f_1 and f_2 of the two laser diodes are slightly detuned, resulting in an amplitude modulation at $\Delta f = f_1 - f_2$ with a modulation depth of 24 %. This modulation frequency can be swept from zero up to several hundreds of GHz by changing the temperature of one of the lasers. The modulated laser light is passed into the experimental insert into a transport dewar by an optical fiber that ends at ≈ 1 mm above the sample position. The temperature at the sample position is controlled by adjustment of the contact gas pressure in the cryostat and a resistive heater placed in the

vicinity of the sample. A bias current is applied by a low-noise current source through the DC path of the bias-tee. The high frquency path is connected to a two-stage low noise amplifier with low power consumption that was designed for cryogenic applications [15]. Then, the pre-amplified signal is led out of the cryostat by a rigid stainless steel high-frequency cable. The response of the sample is measured by an Agilent spectrum analyzer. The read-out electronics limits the system bandwidth to a frequency of 10 GHz.

4. Results and discussion

When a photon is absorbed in a superconducting thin film, its energy $h\nu$ will be quickly redistributed within the electron subsystem by inelastic electron-electron scattering with a time constant τ_{ee}. Since this time is much shorter than the electron-phonon and phonon-electron interaction times (τ_{ep} and τ_{pe}), the electron and phonon subsystems are essentially decoupled. In this quasi-equilibrium condition, each subsystem can be assigned a separate temperature T_e and T_p. After the energy is transferred to the phonons, the heat is then transported out of the film by phonon diffusion and phonon escape to the substrate at bath temperature T_S with the characteristic time constant τ_{es}. It was shown that this process can be well described by the two-temperature (2T) model [4]. If Joule heating produced by an applied bias current can be neglected and only small deviations from the equilibrium are considered, the differential equations of the model can be linearized:

$$\begin{aligned} C_e \frac{dT_e}{dt} &= \frac{\alpha P_{in}(t)}{V} - \frac{C_e}{\tau_{ep}}(T_e - T_{ph}) \\ C_{ph} \frac{dT_{ph}}{dt} &= \frac{C_{ph}}{\tau_{pe}}(T_e - T_{ph}) - \frac{C_{ph}}{\tau_{es}}(T_{ph} - T_S) \end{aligned} \tag{1}$$

where C_e and C_{ph} are the electron and phonon specific heats, respectively, α is the radiation absorption coefficient, V is the volume of the device and $P_{in}(t)$ is the incident optical power.

The change of the electron temperature incurred by the absorbed radiation power can be measured by the change of voltage due to a change of the sample resistance:

$$\Delta U = I_{Bias} \frac{dR}{dT} \Delta T_e \tag{2}$$

For a periodic excitation $P_{in}(t) = P_0 \cos \omega t$, the time evolution of the electron temperature change ΔT_e can be calculated from the 2T model [16]. For low frequencies, the resulting equation can be simplified to a single roll-off function:

$$\Delta U(\Delta f) = \frac{\Delta U(0)}{\sqrt{1 + (\Delta f / f_\varepsilon)^2}} \tag{3}$$

Figure 1 shows the dependence of the signal response on bias current measured at 150 MHz

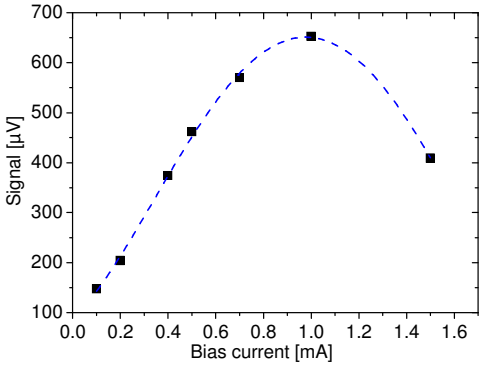

Figure 1. Dependence of the photoresponse of a 22 nm NbN film on bias current at 150 MHz.

modulation frequency for a 22 nm thick NbN sample. For small currents, the signal increases linearly with the bias current as expected from equation (2). The same dependence of the response on bias current was observed for the YBCO samples.

The measurements of the response spectra for NbN and YBCO (figure 2) were obtained at constant biasing current by sweeping the modulation frequency. A clear plateau for the lower frequencies was observed for all samples, followed by a decay at higher frequencies. The parasitic modulation with 500 MHz on top of the signal is caused by impedance mismatch of the samples to the readout circuit. The photoresponse of the YBCO films was for all samples below the values of NbN. The reason is that not only the temperature derivative of the resistance is much lower, but also the absorption coefficient α in the near-infrared wavelengths is higher in NbN compared to YBCO [1], [17]. In addition, due to the larger film thicknesses the volumes of the YBCO samples presented in this report are much larger compared to the samples made from ultra-thin NbN films.

The experimentally measured data is fitted to equation (3), where $\Delta U(0)$ and f_ε are the fitting parameters. The solid lines in figure 2 show these fits for the response spectra measured on NbN and YBCO samples with different thicknesses. From these fits we extracted the characteristic roll-off frequencies f_ε, indicated by arrows in figure 2.

We can directly calculate the energy relaxation time $\tau_\varepsilon = (2\pi f_\varepsilon)^{-1}$ from the frequencies f_ε obtained by the fits. For NbN, we obtain values between 115 ps for the 4.2 nm film and 284 ps for the 22 nm thick film. In case of YBCO, the values range between 512 ps for the 23.5 nm film and 2 ns for the 44 nm film. For both materials the energy relaxation time τ_ε decreases steadily with decreasing film thickness d.

Since in YBCO the heat capacity of the phonons C_{ph} is much larger than that of the electrons C_e by a factor of 38, the bolometric and electron processes are indeed strongly decoupled. The phonon diffusion can be neglected for these films since the phonon mean free path l_{ph} is much larger than the film thickness. In this case, we can assume that the relaxation processes are only due to the heat transport performed by phonons crossing the thermal boundary from the film into the substrate, so that $\tau_\varepsilon = \tau_{es}$. However, for NbN where the ratio C_{ph}/C_e is much smaller (6.5 for T=4.2K), the observed energy relaxation time τ_ε is a combination of both escape time and electron-phonon interaction and can be expressed as $\tau_\varepsilon = \tau_{ep} + (1 + C_e/C_{ph})\tau_{es}$.

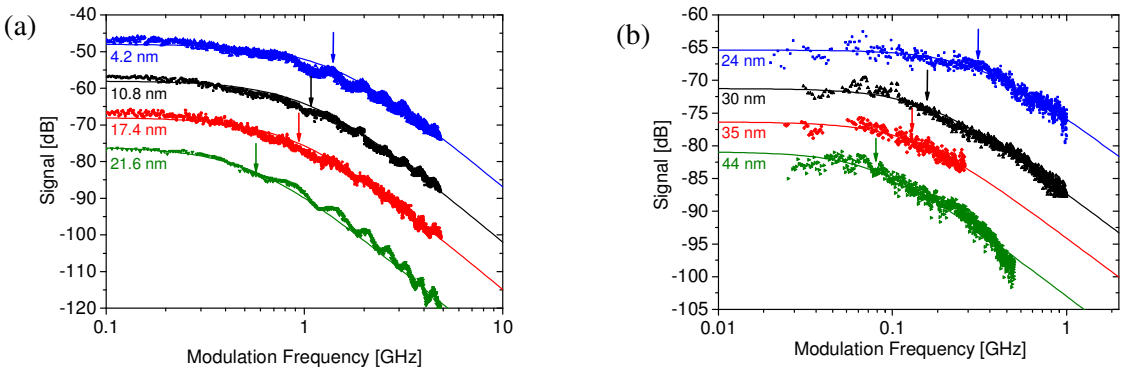

Figure 2. Dependence of voltage response on amplitude-modulated optical (λ=850 nm) radiation for (a) NbN and (b) YBCO samples with different film thicknesses indicated in the graph. The graphs are shifted in y-direction for better comparison. The solid lines are fits of formula (3) to the spectra. The roll-off frequencies f_ε are indicated by arrows.

5. Conclusion

A systematic study of energy relaxation processes in thin NbN and YBCO films with different thicknesses deposited on sapphire substrates has been performed using the frequency domain technique at optical wavelengths. Although the two materials are very different in their physical properties and are operated at different temperature ranges, we succeeded to measure samples in the same measurement setup. We found that due to the steepness of the transition d*R*/d*T* and the very different operating conditions, the response of the YBCO samples was much lower than that of NbN for comparable film thicknesses.

Response spectra for modulation frequencies between 10 MHz and 10 GHz were measured and the characteristic energy relaxation time τ_ε was extracted. For both materials we observed a clear decrease of τ_ε with decreasing film thickness. According to the 2T model, we can argue that the energy relaxation time τ_ε measured for the YBCO samples is due to phonon escape from the film into the substrate, i.e. $\tau_{es,}$ allowing us to get direct information on the phonon spectra in these films. YBCO films of 24 nm to 44 nm thickness gave τ_{es} values of 0.5 ns to 2.0 ns, correspondingly. However, for NbN, we expect that τ_ε is a mixture of τ_{es} and τ_{ep} and found values between 115 ps to 284 ps for 3 nm to 22 nm thick films, respectively.

Acknowledgements

The authors would like to thank H. Wermund and K. Gutbrod for their help in creating the experimental setup as well as A. Stassen for the sample preparation. This work was supported in part by the Karlsruhe School of Optics and Photonics (KSOP) and by the DFG Center of Functional Nanostructures.

References

[1] Danerud M, Winkler D, Lindgren M, Zorin M, Trifonov V, Karasik B S, Gol'tsman G N and Gershenzon E M 1994 *J. Appl. Phys.* **76** 1902-9

[2] Il'in K S, Lindgren M, Currie M, Semenov A D, Gol'tsman G N, Sobolewski R, Cherednichenko S I and Gershenzon E M 2000 *Appl. Phys. Lett.* **76** 2752-4

[3] Sergeev A V, Semenov A D, Kouminov P, Trifonov V, Goghidze I G, B. Karasik S, Gol'tsman G N and Gershenzon E M 1994 *Phys. Rev.* B **49** 9091-6

[4] Semenov A D, Nebosis R S, Gousev Yu P, Heusinger M A and Renk K F 1995 *Phys. Rev.* B **52**, 581-9

[5] Lindgren M, Currie M, Williams C, Hsiang T Y, Fauchet P M, Sobolewski R, Moffat S H, Hughes R A, Preston J S and Hegmann F A 1999 *Appl. Phys. Lett.* **74** 853-5

[6] Kooi J W, J. Baselmans J A, Hajenius M, Gao J R, Klapwijk T M, Dieleman P, Baryshev A and de Lange G 2007 *J. Appl. Phys.* **101**, 044511

[7] Cherednichenko S, Drakinskiy V, Baubert J, Krieg J-M, Voronov B, Gol'tsman G and Desmaris V 2007 *J. Appl. Phys.* **101**, 124508

[8] Il'in K S and Siegel M 2002 *J. Appl. Phys.* **92** 361-9

[9] Harnack O, Il'in K S, Siegel M, Karasik B S, McGrath W R and de Lange G 2001 *Appl. Phys. Lett.* **79** 1906-8

[10] Semenov A D, Il'in K S, Siegel M, Smirnov A, Pavlov S, Richter H and Hübers H-W 2006 *Supercond. Science and Technol.* **19** 1051-6

[11] Semenov A, Haas P, Hübers H.-W., Ilin K, Siegel M, Kirste A, Drung D, Schurig T and Engel A 2009 *Journal of Modern Optics* **56** 345-51

[12] Il'in K S, Stockhausen A, Siegel M, Semenov A D, Richter H and Hübers H-W 2008 *19th Int. Symp. On Space Terahertz Technology* 403-8

[13] Il'in K S, Stockhausen A, Scheuring A, Siegel M, Semenov A D, Richter H and Hübers H-W 2009 *IEEE Trans. On Appl. Supercond.* **19**, 269-73

[14] TOPTICA Photonics, *www.toptica.com*

[15] Wuensch S, Ortlepp T, Crocoll E, Uhlmann F H and Siegel M 2009 *IEEE Trans. On Appl. Supercond.* **19** 574-79
[16] Perrin N and Vanneste C 1983 *Phys. Rev.* B **28** 5150-9
[17] Semenov A, Günther B, Böttger U Hübers H-W Bartolf H Engel A Schilling A Ilin K Siegel M Schneider R Gerthsen D and Gippius N A 2009 *Phys Rev* B **80** 054510